Antiferromagnetic order in the quasicrystal approximant Cd_{6}Tb studied by x-ray resonant magnetic scattering

M. G. Kim, G. Beutier, A. Kreyssig, T. Hiroto, T. Yamada, J. W. Kim, M. de Boissieu, R. Tamura, and A. I. Goldman

Phys. Rev. B **85**, 134442 — Published 24 April 2012

DOI: 10.1103/PhysRevB.85.134442

Antiferromagnetic order in the quasicrystal approximant, Cd_6Tb, studied by x-ray resonant magnetic scattering

M. G. Kim[1], G. Beutier[2], A. Kreyssig[1], T. Hiroto[3], T. Yamada[3], J. W. Kim[4], M. de Boissieu[2], R. Tamura[3], and A. I. Goldman[1]
[1]*Ames Laboratory, U. S. DOE and Department of Physics and Astronomy, Iowa State University, Ames, Iowa 50011, USA*
[2]*SiMAP, Grenoble - INP CNRS UJF, Boîte Postale 75, 38402 Saint Martin d'Hères, France*
[3]*Department of Materials Science and Technology, Tokyo University of Science, Noda, 278-8510, Japan and*
[4]*Advanced Photon Source, Argonne National Laboratory, Argonne, Illinois 60439, USA*
(Dated: March 7, 2012)

We have used x-ray resonant magnetic scattering at the Tb L_2 edge to elucidate the nature of magnetic ordering in Cd_6Tb, a 1/1 approximant closely related to the *R*-Mg-Cd (*R* = rare earth) icosahedral alloys. Below $T_N \approx 24$ K, the ordered moments associated with the icosahedral clusters at the corner and body-center of the pseudo-cubic unit cell are antiferromagnetically correlated and long-range magnetic order is realized.

PACS numbers: 75.25.-j, 75.50.Ee, 61.44.Br

I. INTRODUCTION

The possibilities for magnetic ordering in aperiodic crystals have been the subject of intense theoretical and experimental studies since the discovery of icosahedral quasicrystals in 1982.[1] The first generation of Al-*TM* (*TM* = 3*d* transition metal) quasicrystals with moment bearing elements, such as Al-Mn and Al-Pd-Mn, provided some insight into the fate of magnetism in quasiperiodic systems: only a small fraction of the Mn ions carry a moment (at most a few percent), and these moments appear to be distributed randomly on the quasilattice.[2] It is not surprising, then, that long-range magnetic order is not realized in these quasicrystals and their low-temperature ground state is best characterized as a spin-glass.

The discovery of the Zn-Mg-*R* and Cd-Mg-*R* (*R* = rare earth) quasicrystals with sizeable local moments that interact via indirect exchange (i.e. the RKKY interaction) reinvigorated the search for long-range magnetic order in the icosahedral phase.[3–6] However, all of the known quasicrystals with moment bearing elements exhibit frustration and spin-glass-like behavior at low temperature.[7,8] In Zn-Mg-*R* and Cd-Mg-*R*, dc- and ac-susceptibility measurements demonstrate canonical spin-glass behavior.[9,10] Neutron diffraction measurements clearly show the presence of short-range magnetic correlations (diffuse scattering) with overall icosahedral symmetry at low temperature that has been interpreted in terms of strong correlations between moments on individual clusters.[8] Correlations between moments on adjacent spin clusters appear to be absent. Nevertheless, many theoretical treatments of spins on aperiodic lattices support the notion of long-range antiferromagnetic order on a quasilattice.[11–15] To date, however, there has been no experimental confirmation of long-range magnetic order in quasicrystalline systems.

The origin of frustration in aperiodic crystals is itself a much researched topic. For the Zn-Mg-*R* and Cd-Mg-*R* icosahedral alloys, there is strong evidence that the geometry or topology of the quasilattice plays the primary role. For instance, the magnetic rare earth sites in Cd-Mg-*R* correspond to the vertices of the triangular faces of an icosahedron contained within the Tsai-type clusters which form the backbone of the quasicrystal structure.[16,17] Thus situated, the geometrical frustration associated with triangular arrangements of spins follows naturally.

Interestingly, the absence of long-range magnetic order extends to crystalline approximant phases of the icosahedral structures as well. Crystalline approximants are periodic crystals with unit cell atomic decorations that are closely related to the respective quasicrystalline phases.[18] Early studies[19,20] of the magnetic properties of μ-$Al_4Mn_xCr_{1-x}$ provided evidence that, like the Al-Mn and Al-Pd-Mn quasicrystals, only a fraction of the Mn ions carry a moment. However, recent studies of μ-Al_4Mn also indicate that the magnetic frustration may be geometrical in origin arising from the presence of triangular spin clusters in the structure.[21] For rare-earth based approximants, where the exchange is dominated by the long-range RKKY interaction, extensive magnetic property investigations found spin-glass-like freezing of the moments in Ag-In-*R* 1/1 cubic approximants for *R* = Eu, Gd, Tb and Dy.[22] Furthermore, both the Ag-In-Gd icosahedral phase and its 1/1 cubic approximant show similar behavior as both evolve to spin-glasses at low temperature.[23]

Surprisingly, the 1/1 approximant to the Cd-Mg-*R* icosahedral phases, Cd_6R, appears to be an exception to the rule. In particular, recent magnetic susceptibility and specific heat measurements[24–26] indicate the onset of long-range magnetic order at low temperature. The relatively high T_N (24 K) for Cd_6Tb,[24] in addition to the relatively strong resonant enhancement found at the Tb L-edges,[27] make it an obvious candidate for microscopic magnetic structure investigations by XRMS. For Cd_6Tb, at elevated temperatures, the magnetic susceptibility follows a Curie-Weiss law with an effective moment/Tb^{3+} ion (9.8 μ_B), consistent with the free ion value for Tb^{3+}, and a Weiss temperature, Θ = -17 K, signalling that the dominant interactions between the Tb moments are antiferromagnetic. At low temperature, three anomalies are observed at 24, 19 and 2.4 K in the magnetic susceptibility data and corresponding features are found in the specific heat measurements, consistent with magnetic ordering. However, elucidation of the microscopic nature and spatial extent of the magnetic state below 24 K requires scattering measurements. Unfortunately, the naturally occurring isotope mixture of Cd is highly neutron absorbing making magnetic neutron diffraction measurements impossible without the appropriate

isotopic substitution.

Here, we report the results of x-ray resonant magnetic scattering (XRMS) measurements on Cd_6Tb. We demonstrate that long-range antiferromagnetic order is, indeed, realized below T_N = 24±1 K. The Bragg peaks that arise from the antiferromagnetic order are as sharp as those associated with the chemical structure, providing a lower limit for the magnetic correlation length of approximately 500 Å. Viewing the structure as a body-centered cubic (bcc) packing of Tsai clusters, we find that the Tb ions associated with the icosahedral cluster at the corner of the unit cell are antiferromagnetically correlated with the Tb ions associated with the icosahedral cluster at the body-center of the unit cell.

II. EXPERIMENTAL DETAILS

Single crystals of Cd_6Tb were prepared by a self-flux method by melting high-purity elements of Cd (99.9999 wt. %) and Tb(99.9 wt.%) in a 9:1 atomic ratio at 993 K for 24 h in an alumina crucible sealed inside a quartz tube. This was followed by slow cooling at the rate of 2 K/h to 753 K. The remaining Cd melt was then removed by means of a centrifuge and the alloys were subsequently annealed at 923 K for 100 h to improve the sample homogeneity, followed by further annealing at 473 K for 3 weeks to reduce point defects. Single crystals of millimeter size, with well defined facets normal to the [1 0 0] direction, were used for XRMS experiments. The dimensions of the single crystal studied in the XRMS measurements were approximately $3\times1\times1\,\mathrm{mm}^3$. The mosaicity of the crystal, measured for the (10 0 0) charge peak at room temperature, was approximately 0.025 degrees full-width-at-half-maximum (FWHM), attesting to the high quality of the sample.

The XRMS experiment was performed on the 6-ID-B beamline at the Advanced Photon Source at the Tb L_2-edge (E = 8.252 keV). The incident radiation was linearly polarized perpendicular to the vertical scattering plane (σ-polarized) with a beam size of 0.5 mm (horizontal) × 0.2 mm (vertical). In this configuration, dipole resonant magnetic scattering rotates the plane of linear polarization into the scattering plane (π-polarization). Pyrolytic graphite PG(0 0 6) was used as a polarization analyzer to suppress the charge and fluorescence background by roughly a factor of 100 relative to the magnetic scattering signal. The sample was mounted at the end of the cold finger of a closed-cycle refrigerator with the ($H0L$) plane coincident with the scattering plane.

The resonant magnetic diffraction, $I(\psi)$, for the σ-to-π scattering geometry depends upon the component of the magnetic moment along the scattered beam direction and can be written as $I(\mathbf{Q},\,\alpha,\,\beta) \,=\, C\,[\widehat{\mathbf{m}}\cdot\widehat{\mathbf{k}'}(\mathbf{Q})]^2\,A(\mathbf{Q},\,\alpha,\,\beta)$ where C is an overall scale factor that accounts for the resonant scattering matrix element, structure factor and incident beam intensity, $\widehat{\mathbf{m}}$ and $\widehat{\mathbf{k}'}$ represent the magnetic moment and scattered beam directions, respectively, and A accounts for the sample absorption correction.[28] The sample geometry required off-specular scattering measurements of the magnetic peaks. That is, the angle, α, of the incident beam, $\mathbf{k}$, with respect to the sample surface is different from the angle, β, of the outgoing beam, $\mathbf{k}'$, with respect to the sample surface.[29]

III. RESULTS AND DISCUSSION

At room temperature, Cd_6Tb is cubic ($Im\bar{3}$) with the Tb ions found at the 24*g* Wyckoff position with full occupancy. Therefore, the Tb ions can be viewed as occupying the second icosahedron shell of the Tsai clusters situated at the corner and body-centered positions, as described previously,[16,17] and shown in Fig. 1(a). The cubic symmetry distorts these icosahedral clusters only slightly so that eight of the twenty faces form equilateral triangles with an edge length of 5.73 Å (for $a_{\mathtt{cubic}} = 15.439$ Å), and the remaining twelve faces form isosceles triangles with the longer leg (5.84 Å) parallel to the cube edges. The Tb-Tb distance between neighboring clusters along the body diagonal (5.72 Å) is comparable to the intra-cluster distances. Indeed, as shown in Fig. 1(b), the Tb network may alternatively be viewed as a set of corner-sharing tilted octahedra composed of equilateral and isosceles triangles, again emphasizing the geometrical frustration inherent to the structure and the similarity between intra- and inter-cluster Tb-Tb distances and the related magnetic exchange.

Below $T \approx 150$ K, Cd_6Tb undergoes a cubic-to-monoclinic structural transition as a consequence of the ordering of the Cd tetrahedra at the centers of the Tsai clusters.[30] Although the low temperature structure of Cd_6Tb has not yet been fully determined, it is proposed to be isostructural with the low-temperature monoclinic phase of Zn_6Sc.[31] In the low temperature monoclinic phase, with unit cell sides of $\sqrt{2}a_{\mathtt{cubic}} \times a_{\mathtt{cubic}} \times \sqrt{2}a_{\mathtt{cubic}}$ and β = 89.93°, the icosahedra (and octahedra) are distorted further, with Tb-Tb separations ranging from approximately 5.5 Å to 6.0 Å. This additional distortion likely modifies the magnetic exchange interactions sufficiently to enhance magnetic ordering.

Although the magnetic structure of Cd_6Tb must ultimately be referenced to the low-temperature structure, for our purposes here, we will discuss the magnetic structure in terms of the high temperature bcc arrangement of Tb icosahedra. The indices of allowed charge reflections must satisfy the condition: $H + K + L = 2n$, where n is an integer. Upon cooling the sample through the cubic-to-monoclinic structural transition at $T_S \approx 150$ K, the charge peaks split and a collection of peaks that arise from different domains within the illuminated volume of the sample are observed as shown in Figs. 2(a)-(d) for the (14 0 0) charge peak. The relative intensities of different sub-peaks reflect, in part, the relative populations of the different domains within the illuminated volume. For the proposed C2/c symmetry of the monoclinic phase, reflections with $H + K + L = 2n+1$ remain forbidden (the centering is preserved by the phase transition).

For temperatures above $T_N \approx 24$ K, only Bragg peaks consistent with the chemical structure of Cd_6Tb were observed. However, below T_N, additional Bragg scattering appeared at points in reciprocal space corresponding to odd values of the sum, $H + K + L = n$ (for n odd) as illustrated in Figs. 2(e)-(h) which also shows that magnetic peaks arise from all domains

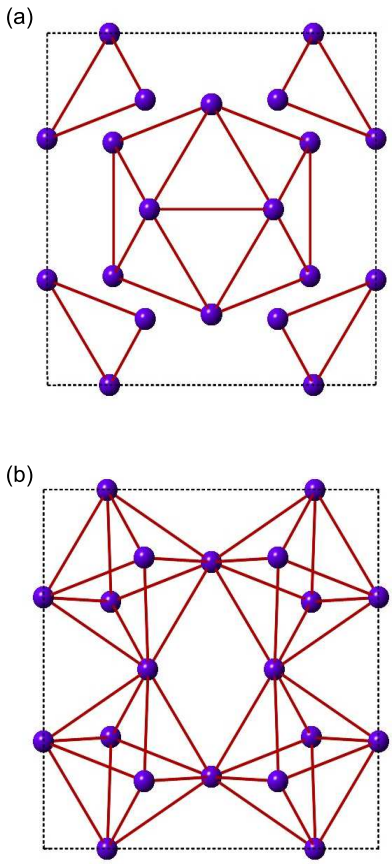

FIG. 1: (Color online) Arrangement of Tb ions in the high-temperature cubic unit cell of Cd_6Tb viewed along one of the cubic axes. The network of Tb ions can be viewed either as a bcc packing of icosahedra as in (a) or a set of corner-sharing tilted octahedra as in (b).

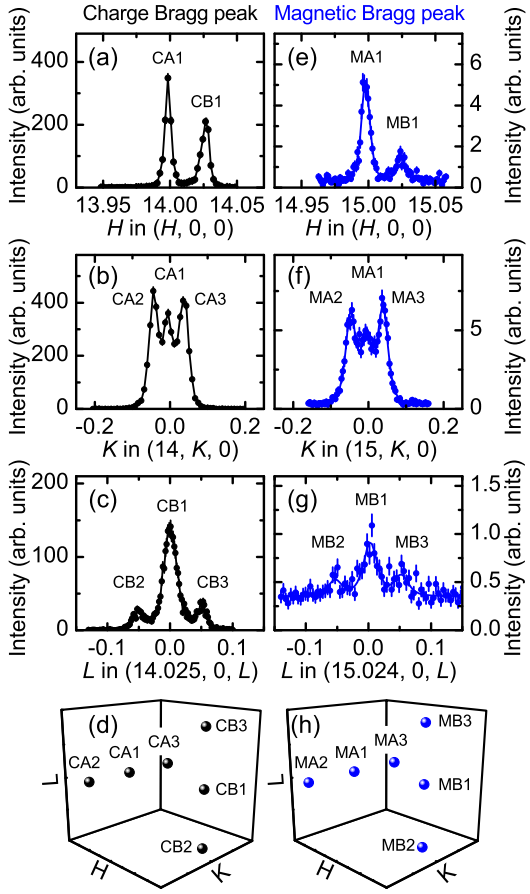

FIG. 2: (Color online) Distribution of charge and magnetic peaks measured by an (a) H-scan, (b) K-scan and (c) L-scan through the (14 0 0) charge peak position and an (e) H-scan, (f) K-scan and (g) L-scan through the (15 0 0) magnetic peak position. Panels (d) and (h) plot the charge and magnetic peak positions schematically.

associated with the chemical structure. Furthermore, we see that the magnetic peaks are as sharp as the charge peaks, confirming that there is long-range magnetic order in Cd_6Tb below T_N and suggesting that the magnetic correlation length is limited by the finite size of the monoclinic domains. Taking the magnetic correlation length to be given by $\xi_m \approx \frac{\pi}{\Delta\, q_m}$, where $\Delta\, q_m$ is the longitudinal half-width-at-half-maximum of the magnetic diffraction peak, we find $\xi_m \geq 500$Å.

In terms of the bcc unit cell description of Cd_6Tb, the antiferromagnetic order breaks the body-centering translational symmetry of the chemical unit cell such that the Tb ions associated with the icosahedral cluster at the corner of the unit cell are antiferromagnetically correlated with the Tb ions associated with the icosahedral cluster at the center of the unit cell. A complete specification of magnetic structure, including the magnetic arrangement within the clusters themselves, will first require a complete description of the chemical structure in the low-temperature monoclinic phase as well as the details of the monoclinic domain structure. Further analysis of the magnetic structure can then clarify whether the Tb moments are collinearly aligned or arranged in a more complex manner.

The magnetic origin of the scattering at $H + K + L = n$ (for n odd) was confirmed by the resonance feature observed in the energy scans through the Tb L_2 absorption edge (Fig. 3). The energy scan Fig. 3 in the σ-to-π scattering channel was performed with the resolution of the diffractometer relaxed (slits opened) in order to integrate over all of the magnetic scattering around the (9 0 0) magnetic peak position, and is typical of resonant magnetic scattering at the L edges of rare-earth compounds.[27] At the L_2 edge of rare-earth elements, the resonance primarily involves electric dipole ($E1$) transitions from the $2p_{\frac{1}{2}}$ core level to the empty $5d$ states, seen as the strong line just at, or slightly below, the maximum in the measured fluorescence intensity. For the rare earth compounds, the $5d$ bands are spin-polarized through their interaction with the localized $4f$ moments and, therefore, reflect the magnetization density distribution of the lattice. Energy scans were also done in the σ-to-σ scattering channel which is sensitive to the charge, rather than the resonant magnetic, contributions to the scattering and no diffraction peaks were found at the magnetic peak positions.

The temperature dependence of the magnetic scattering was

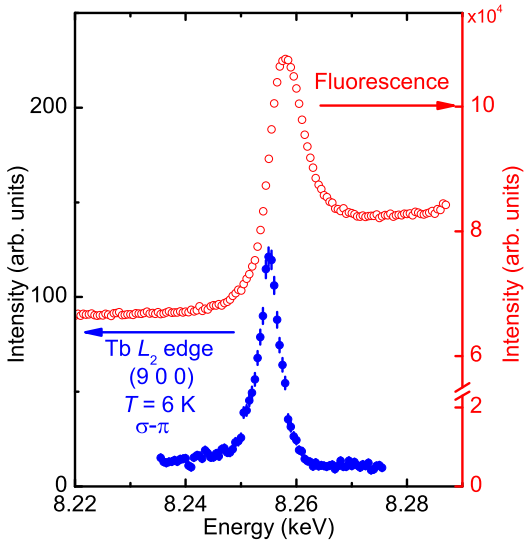

FIG. 3: (Color online) The fluorescence (open circles) and magnetic intensity (closed circles) measured around the (9 0 0) magnetic peak as a function of incident beam energy through the Tb L_2 edge at T = 6 K.

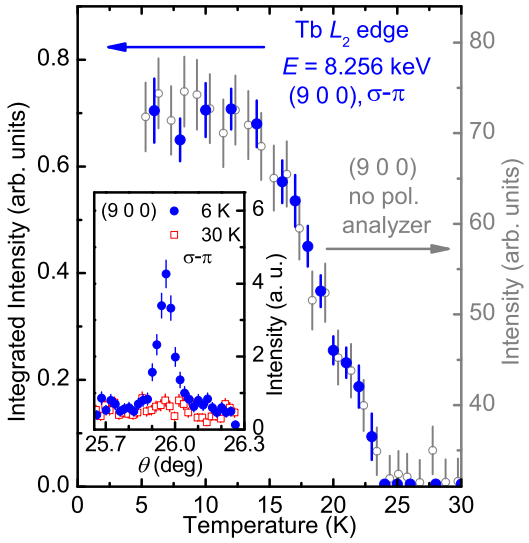

FIG. 4: (Color online) The temperature dependence of the magnetic peak intensity measured without an analyzer (open circles) and integrated intensity (filled circles) measured with polarization analysis at the (9 0 0) magnetic peak position referenced to the cubic unit cell. The inset shows the magnetic peak at T = 6 K and its absence at 30 K (above T_N).

measured at several magnetic peaks, and is shown for the (9 0 0) magnetic peak in Fig. 4. The magnetic order parameter was also measured using relaxed resolution to integrate over the distribution of peaks at the (9 0 0) magnetic Bragg position. The open circles represent the peak intensity measured as the sample temperature was increased during a temperature scan in the absence of the polarization analyzer. These data were supplemented by measurements of the integrated intensity (solid circles) of the (9 0 0) magnetic Bragg peak at selected temperatures, with polarization analysis, as the sample was rocked through the reflection condition. The measured Néel temperature, T_N = 24±1 K is consistent with that found from bulk susceptibility and specific heat measurements[24] and, again, confirms the magnetic origin of the Bragg scattering at (9 0 0). We further note that there is an apparent kink in the evolution of the magnetic order as the temperature is decreased below about 19 K. This temperature corresponds to the lower temperature feature observed in the susceptibility and specific heat measurements and may arise from either a change in the magnetic structure (e.g. a reorientation of the moment directions) or, perhaps, from additional contributions to the ordered moment from Tb ions that order below T_N. The lowest temperature transition observed in the bulk measurements at 2.4 K was beyond the range of the displex cryostat employed for these measurements.

IV. CONCLUSIONS

Summarizing our results, using XRMS we have shown that Cd_6Tb, a 1/1 crystalline approximant to the Cd-Mg-*R* icosahedral quasicrystals, manifests long-range antiferromagnetic order below T_N = 24±1 K. The magnetic correlation length is in excess of 500 Å and comparable to that measured for the chemical structure which is possibly limited by the finite size of the monoclinic domains. In terms of the high-temperature bcc unit cell description, the antiferromagnetic order breaks the body-centering translational symmetry of the chemical unit cell such that the Tb ions associated with the icosahedral cluster at the corner of the unit cell are antiferromagnetically correlated with the Tb ions associated with the icosahedral cluster at the center of the unit cell.

The appearance of long-range magnetic order in this crystalline approximant, in contrast to the spin-glass behavior observed for quasicrystals and other, related, approximant phases calls for further experimental and theoretical study. Differences in the nearest-neighbor exchange interactions above and below the structural transition likely play an important role in promoting long-range magnetic order. However, one must also consider, for example, the extended range of the RKKY interaction, as well as the effects of the crystalline electric field associated on the $4f$ local moments. Therefore, detailed structural and XRMS studies of other Cd_6R approximants are called for. In closing, we note that these approximant phases offer an unprecedented opportunity for understanding the potential for magnetic ordering in quasicrystalline materials.

We acknowledge valuable discussions with J. C. Lang. Work at the Ames Laboratory was supported by the Division of Materials Sciences and Engineering, Office of Basic Energy Sciences, U. S. Department of Energy under Contract No. DE-AC02-07CH11358. Work at the Tokyo University of Science was supported by KAKENHI (Grant No. 20045017) from the ministry of Education, Culture, Sports, Science Technology of Japan. Use of the Advanced Photon Source was supported by the U. S. DOE under Contract No.

DE-AC02-06CH11357.

[1] D. Shechtman, I. Blech, D. Gratias, and J. W. Cahn, Phys. Rev. B **53**, 1951 (1984).
[2] F. Hippert and J. J. Préjean, Phil. Mag **88**, 2175 (2008).
[3] Z. Luo, S. Zhang, Y. Tang, and D. Zhau, Scr. Metall Mater. **28**, 1513 (1993).
[4] A. P. Tsai, A. Niikura, A. Inoue, T. Masumot, Y. Nishida, K. Tsuda, and M. Tanaka, Phil. Mag. Lett. **70**, 169 (1994).
[5] J. Q. Guo, E. Abe, and A. P. Tsai, Jpn. J. Appl. Phys., Part 2 **39**, L770 (2000).
[6] J. Q. Guo, E. Abe, and A. P. Tsai, Phil. Mag. Lett. **81**, 17 (2001).
[7] K. Fukamichi, *Physical Properties of Quasicrystals* (Springer-Verlag, Berlin, 1999), pp. 295–326.
[8] T. J. Sato, Acta Crystallogr., Sect A: Found. Crystallogr. **61**, 39 (2005).
[9] I. R. Fisher, K. O. Cheon, A. F. Panchula, P. C. Canfield, M. Chernikov, H. R. Ott, and K. Dennis, Phys. Rev. B **59**, 308 (1999).
[10] S. E. Sebastian, T. Huie, I. R. Fisher, K. W. Dennis, and M. J. Kramer, Phil. Mag **84**, 1029 (2004).
[11] R. Lifshitz, Phys. Rev. Lett. **80**, 2717 (1998).
[12] R. Lifshitz, Mat. Sci. and Eng. **294-296**, 508 (2000).
[13] S. Wessel, A. Jagannathan, and S. Haas, Phys. Rev. Lett. **90**, 177205 (2003).
[14] E. Y. Vedmedenko, U. Grimm, and R. Wiesendanger, Phys. Rev. Lett. **93**, 076407 (2004).
[15] S. Matsuo, S. Fujiwara, H. Nakano, and T. Ishimasa, J. Non-Cryst. Solids **334-335**, 421 (2004).
[16] C. P. Gómez and S. Lidin, Phys. Rev. B **68**, 124203 (2003).
[17] S. Y. Piao, C. P. Gómez, and S. Lidin, Z. Naturforscg., B:Chem Sci. **61b**, 644 (2006).
[18] A. I. Goldman and K. F. Kelton, Rev. Mod. Phys. **65**, 213 (1993).
[19] T. Schenk, H. Klein, M. Audier, V. Simonet, F. Hippert, J. Rodriguez-Caravajal, and R. Bellisent, Phil. Mag. Lett. **76**, 189 (1997).
[20] V. Simonet, F. Hippert, M. Audier, and G. T. de Laissardière, Phys. Rev. B **58**, R8865 (1998).
[21] S. Jazbec, Z. Jagličić, Z. Vrtnik, M. Wencka, M. Feuerbacher, M. Heggen, S. Roitsch, and J. Dolinšek, J. Phys.:Condens. Matter **23**, 045702 (2011).
[22] S. Ibuka, K. Iida, and T. J. Sato, J. Phys.:Condens. Matter **23**, 056001 (2011).
[23] P. Wang, Z. M. Stadnik, K. al Qadi, and J. Przewoźnik, J. Phys.:Condens. Matter **21**, 436007 (2009).
[24] R. Tamura, Y. Muro, T. Hiroto, K. Nishimoto, and T. Takabatake, Phys. Rev. B **82**, 220201(R) (2010).
[25] R. Tamura, Y. Muro, T. Hiroto, H. Yaguchi, G. Beutier, and T. Takabatake, Phys. Rev. B **85**, 014203 (2012).
[26] A. Mori, H. Ota, S. Yoshiuchi, K. Iwakawa, Y. Taga, Y. Hirose, T. Takeuchi, E. Yamamoto, Y. Haga, F. Honda, et al., J. Phys. Soc. Jpn. **81**, 024720 (2012).
[27] J. W. Kim, Y. Lee, D. Wermeille, B. Sieve, L. Tan, S. L. Bud'ko, S. Law, P. C. Canfield, B. N. Harmon, and A. I. Goldman, Phys. Rev. B **72**, 064403 (2005).
[28] C. Detlefs, A. H. M. Z. Islam, A. I. Goldman, C. Stassis, P. C. Canfield, J. P. Hill, and D. Gibbs, Phys. Rev. B **55**, R680 (1997).
[29] H. You, J. Appl. Cryst. **32**, 614 (1999).
[30] R. Tamura, K. Edagawa, K. Shibata, K. Nishimoto, S. Takeuchi, K. Saitoh, M. Isobe, and Y. Ueda, Phys. Rev. B **72**, 174211 (2005).
[31] T. Ishimasa, Y. Kasano, A. Tachibana, S. Kashimoto, and K. Osaka, Phil. Mag **87**, 2887 (2007).